# DESIGN CONCEPT FOR AN ALTERNATIVE HEAVY VEHICLE SLIP CONTROL BRAKE ACTUATOR



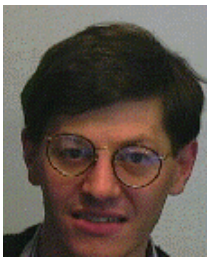

**Jonathan MILLER**
Cambridge University
Cambridge, United Kingdom

**Frank KIENHOFER**
University of the Witwatersranc
South Africa

**David CEBON**
Cambridge University
Cambridge, United Kingdom

**Abstract**
Heavy vehicles have sluggish pneumatic brake actuators that limit the cycling bandwidth of their antilock braking systems. In order to implement more effective braking controllers, the conventional actuation systems must be redesigned. This paper introduces a novel actuator that features high bandwidth, binary actuated valves placed directly on the brake chamber. A preliminary look at the effect of slip control bandwidth on the compromise between stopping distance and air usage is first presented. One-dimensional flow theory is then combined with simple thermodynamic arguments to describe charging and discharging of a brake chamber. The resulting equations are linearized and used to design a closed-loop pressure controller for the actuator. Finally, the performance of the valves is presented with respect to their steady-state accuracy and time delay.

**Keywords:** Wheel slip control, Pneumatic actuator, Heavy vehicles, Brakes, Pulse width modulation, One-dimensional Flow

**Résumé**
Les véhicules lourds ont des actionneurs de freins pneumatiques qui manquent de vigueur, et limitent l’efficacité des ABS (système anti-patinage). Pour permettre une implémentation plus efficace des contrôleurs de freins, les systèmes conventionnels d'actionnement doivent être repensés. Cet article présente un actionneur novateur à large bande avec des valves actionnées en mode binaire et placées directement sur la chambre du frein. L'effet d'une perte de contrôle de la bande passante sur le compromis entre la distance d'arrêt et l'utilisation d'air est présenté en premier lieu. Ensuite, la théorie des fluides uni-dimensionels est combinée à un simple énoncé de thermodynamique pour décrire la charge et la décharge de la chambre du frein. Les équations résultantes sont linéarisées et utilisées pour la conception d'un contrôleur de pression à boucle-fermée pour l'actionneur. Finalement, la performance des valves est présentée en tenant compte de leur précision en régime stationnaire et de leur temps de propagation.

**Mots-clés:** Système Anti-Patinage (ABS), Actionneur Pneumatique, Véhicules Lourds, Freins, Modulation d’Impulsions en Largeur, Théorie des Fluides Uni-Dimensionel.

## 1. Motivation for Investigating Slip Control and Alternative Actuators

Heavy Goods Vehicles (HGV's) have considerably lower maximum retardation rates than passenger cars (Dugoff et al., 1971), (Werde, Decker, 1992), and take 40% more distance for braking on dry roads, contributing to their higher rate of involvement in fatal accidents than any other road vehicles (Peeta et al., 2005), (Annon, 2006). The US National Highway Traffic Safety Administration (NHTSA) believes that improving the discrepancy in stopping distances between cars and trucks is very important towards reducing truck-related fatalities (Dunn, Hoover, 2004). The mandatory use of anti-lock braking systems (ABS) on air braked vehicles in North America and Europe has mitigated this problem somewhat. However, current heavy vehicle ABS uses an inefficient heuristic control approach, which works on cycles of predicting and superseding the limits of tyre-road adhesion, and then reducing brake pressure to allow the wheel to rotate again (Kienhofer, Cebon, 2004). The fill and dump process uses a lot of air, which requires energy to generate and heavy reservoirs for storage.

An alternative approach to ABS is wheel-slip control, which optimizes wheel slip continuously during braking, thereby maximizing deceleration while maintaining vehicle maneuverability. Preliminary estimations with a proof-of-concept control system and vehicle simulation predict reductions of up to 25% in braking distance relative to conventional ABS (Kienhofer, Cebon, 2004). Moreover, since only small adjustments are made to keep the wheel at the optimum slip point, slip control may reduce compressed air consumption. In Kienhofer et. al. (2007), a gain-scheduled slip controller was combined with conventional ABS hardware in a Hardware-in-the-Loop (HiL) rig. The controller gains were scheduled to speed and were designed with loop shaping to ensure satisfactory stability margins.

The gain-scheduled slip control system was very slow, taking nearly a second to rise to the optimal slip point. This resulted in poor deceleration at the start of the stopping event, where speed is highest, producing stopping distances that were 10% higher than conventional ABS. The source of the poor response was the sluggish conventional control valves. Compressibility of air, long pipe lengths, chamber filling time, and valve response time created delays that limit the bandwidth of pneumatic actuators (Bu, Tan, 2007), making HGV actuators harder to control (Jiang, Gao, 2001), (Kawabe et al., 1997), and preventing the use of high gains. These issues are also what limit HGV ABS to working frequencies of 1-2 Hz, compared to passenger cars, which cycle closer to 6-8 Hz (Emereole, 2003), (Bowman, Law, 1993).

There is considerable literature concerned with reducing lags and the speed of response in pneumatic braking systems to improve controllability and stopping distances (Dugoff, Murphy, 1971), (Decker et al., 1986), (Palkovics, Fries, 2001). Recommendations have been made towards using faster electronic valves, shorter signal run times, and putting control valves near the object they are controlling (Murphy et al., 1970), (Decker et al., 1986). However, there has been little published on advanced braking hardware for air braked vehicles since the introduction of Electronic Braking Systems (EBS) by Werde and Decker (1992).

This paper discusses the use of fast pneumatic valves mounted directly on the brake chamber. It focuses on developing closed-loop pressure control of a chamber using such an actuator.

## 2. Theoretical Study of High-Bandwidth Controllers

Kienhofer et al. (2007) simulated a truck with ABS based on wheel-slip control, using fast-

acting pneumatic valves mounted directly on the brake chambers. The vehicle model was subjected to road surface roughness causing fluctuations in vertical tyre forces. The ABS controlled the slip to a target value using a simple PID control loop on a realistic (validated) model of the vehicle, tyres, and brake actuation system.

Figure 1 plots the results of a parametric study with the aforementioned simulation of the effect of controller bandwidth on the compromise between stopping distance and air usage. Results are presented for a 'good' road with an International Roughness Index (IRI) = 2.5 m/km, and a 'poor' road with an IRI = 5 m/km. The stopping distance and compressed air usage are normalized using simulated results for a conventional ABS system.

The simulations illustrate that care should be exercised in controller design. If the bandwidth is too high, the controller will correct for small disturbances about the optimal slip point, yielding marginal benefits in braking distance, but large increases in air usage that risk depleting the supply tank. If the bandwidth is too low, the slip controller will not regulate the wheel slip effectively.

The overall performance can be optimised by calculating a cost function, *J,* which is a combination of air consumption, *C,* and stopping distance, *D,*

$$J = K_1 C + K_2 D \tag{1}$$

where $K_1$ and $K_2$ are conversion factors in units of currency/mass and currency/distance, respectively. A contour of constant $J$ plots as a straight line with gradient $-K_2 / K_1$ on Figure 1. The objective of the design is to drive the operating point downwards perpendicular to this line so as to reduce both *C* and *D*.

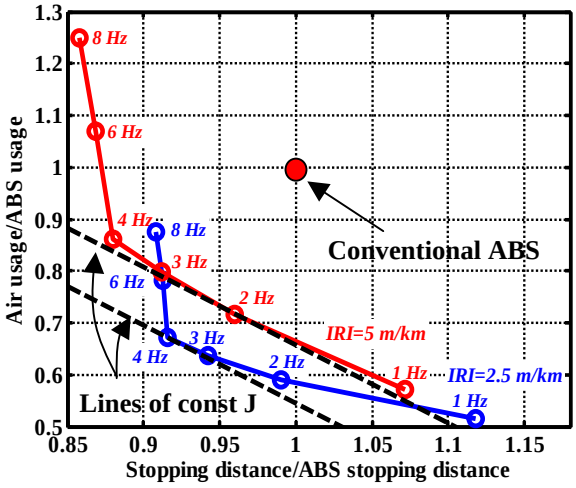


**Figure 1 –** Conflict Diagram Analysis of Air Usage versus Stopping Distance for a Simulated Slip-Control System Operating on Roads with Two Different Surface Roughness Levels

The optimum point on the curves depends on the weightings, $K_1$ and $K_2$. Based on a weight savings analysis done by Fu and Cebon (2003) and an analysis on speed versus accident rate by Kloeden et al. (2002), a value of $K_2 / K_1 = 1.5$ m/kg was determined for the cost function gradient. Using this cost function, the best performing actuator bandwidths are in the range of 2 to 4 Hz (Figure 1).

## 3. Prototype Brake Manifold

A prototype, proof-of-concept brake manifold with integrated, high-bandwidth, 'binary-actuated' valves has been developed in association with Camcon Technology Ltd (Figure 2). The valves operate bi-stably in either the fully-open or fully-closed states, with permanent magnets holding each valve in a given state. A short electrical pulse alters the magnetic field, causing the valve seat to snap to the opposing state with the help of a mechanical spring.

Two valve architectures are used: the Camcon 'Vibrator', which is fast acting (200 μs to switch states) but limited to a 1.5 mm diameter orifice; and the Camcon 'Pushpull,' which is slower (2 ms to switch states), but has an orifice diameter of 3.5 mm. In the prototype system, two Camcon Pushpull valves are used for the inlet and two for the outlet, allowing for rapid charging and discharging of the brake chamber. One fast acting Vibrator valve is also used at the inlet and outlet, respectively, to make small adjustments to keep the braked wheel at the required slip set point and minimize air usage. The Pushpull valves are controlled using a 20 Hz pulse-width modulated (PWM) signal and the Vibrators use a 250 Hz signal.

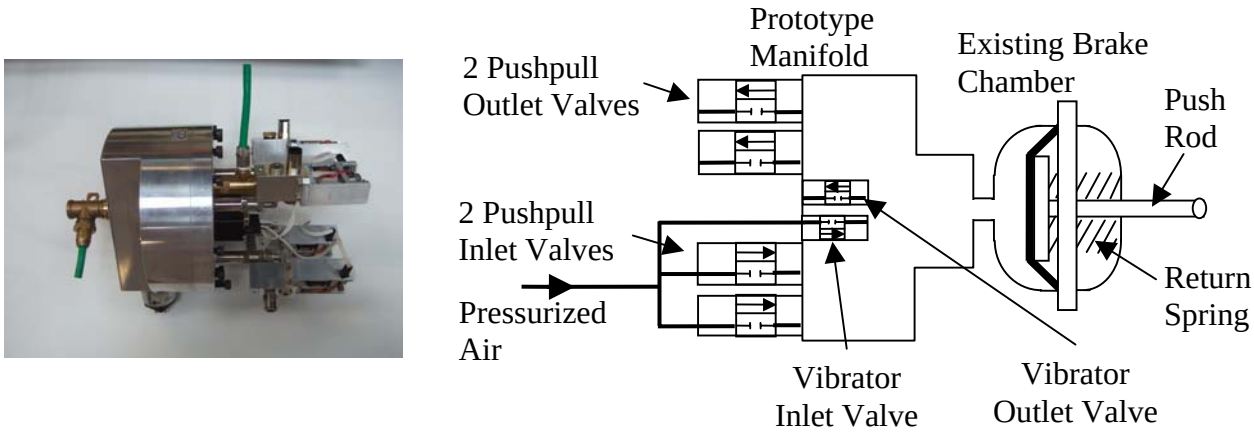


**Figure 2 –** Prototype High Bandwidth Valves and Manifold.

## 4. Characterizing the Prototype Actuator's Pneumatic Response

Characterization of the actuator's response follows the work by Richer and Hurmuzlu (2000), and Subramanian et al. (2004). Assuming air is an ideal gas, heat transfer from the valve orifices is negligible, and shear forces on the walls of the orifices are negligible; the mass flow rate of air through the valves, $\dot{m}_{valve}$, can be described using one-dimensional flow theory:

$$\dot{m}_{valve} = (MS) C_f A_v C_1 \frac{P_u}{\sqrt{T}} \qquad \text{if } \frac{P_d}{P_u} \le P_{cr} \tag{2}$$

$$\dot{m}_{valve} = (MS) C_f A_v C_2 \frac{P_u}{\sqrt{T}} \left(\frac{P_d}{P_u}\right)^{\frac{1}{\gamma}} \sqrt{1-\left(\frac{P_d}{P_u}\right)^{\frac{\gamma-1}{\gamma}}} \qquad \text{if } \frac{P_d}{P_u} \ge P_{cr} \tag{3}$$

where

$$C_1 = \sqrt{\frac{\gamma}{R}\left(\frac{2}{\gamma+1}\right)^{\frac{\gamma+1}{\gamma-1}}}; \qquad C_2 = \sqrt{\frac{2\gamma}{R(\gamma-1)}}; \qquad P_{cr} = \left(\frac{2}{\gamma+1}\right)^{\frac{\gamma}{\gamma-1}} \tag{4}$$

In Equations (2) – (4), *MS* denotes the mark-space ratio of the signal to the valves, which can vary between 0 and 1, $C_f$ is the discharge coefficient, $A_v$ is the valve cross-sectional area, $\gamma$ is the specific heat ratio, $R$ is the specific gas constant, $T$ is the absolute temperature, and $P$ denotes the absolute pressure. The subscripts *'u'* and *'d'* indicate upstream and downstream conditions respectively, and $P_{cr}$ is the critical pressure ratio. Including *MS* in Equations (2) and (3) assumes that the transient buildup of airflow through the valves is fast with respect to the valve switching speed.

The flow of air through the actuator will either be choked (Equation (2)), when the local air velocity through the valve is equal to the speed of sound, or nonchoked (Equation (3)), when the local air velocity is slower than the speed of sound. Air flow through the outlet valves discharges to atmosphere and will predominantly be choked, while the flow through the inlet valves can become nonchoked close to the operating point, depending on the supply tank pressure.

To validate the above theory, the valves were individually connected to a high-pressure upstream supply tank and either discharged to atmosphere, or to a medium pressure downstream supply tank. The mass flow rate through the valves was deduced from pressure changes in the upstream tank, using an equation independent from Equations (2) and (3).

The first law of thermodynamics for unsteady flow in and out of the upstream supply tank is (Richer, Hurmuzlu, 2000):

$$\dot{Q}_{cv} - \dot{W}_{cv} = \dot{m}_{out} h_{out} - \dot{m}_{in} h_{in} + \dot{U}_{cv} \tag{5}$$

where $Q$ is heat transfer, $W$ is work, $h$ is the specific enthalpy, $U$ is internal energy, $m$ is mass, and the subscripts *'in'*, *'out'*, and *'cv'* denote conditions entering, leaving, and within the control volume (the upstream tank) respectively. It is know that,

$$\dot{U}_{cv} = \frac{d}{dt}\left(C_v m T\right)_{cv} = \frac{1}{\gamma - 1}\left(V\dot{P} + P\dot{V}\right)_{cv}; \qquad \dot{W}_{cv} = \left(P\dot{V}\right)_{cv}; \qquad \frac{C_v}{R} = \frac{1}{\gamma - 1} \tag{6}$$

where $t$ is time, $C_v$ is the specific heat at constant volume, $P$ is pressure, and $V$ is volume. Substituting (6) into (5) and rearranging,

$$\dot{Q}_{cv} + \frac{\gamma}{\gamma - 1} R(\dot{m}_{in} T_{in} - \dot{m}_{out} T_{out}) = \frac{1}{\gamma - 1}\left(V\dot{P}\right)_{cv} + \frac{\gamma}{\gamma - 1}\left(P\dot{V}\right)_{cv} \tag{7}$$

Air was discharged through the valves for approximately a second, the duration kept short to minimize heat flow. Consequently, the test can be approximated as adiabatic ($\dot{Q}$ = 0). In addition, if it is assumed that the inflow and outflow temperatures are equal to the control volume temperature, Equation (7) becomes

$$(\gamma \dot{m}_{in} - \gamma \dot{m}_{out}) = \frac{V\dot{P}}{RT} + \frac{\gamma P\dot{V}}{RT} \tag{8}$$

Since the upstream tank is rigid, $\dot{V}$ = 0. Moreover, there is no flow into the tank ($\dot{m}_{in}$ = 0). So, $\dot{m}_{valve}$ can be equated to the mass flow rate out of the tank,

$$\dot{m}_{valve} = -\frac{V_u \dot{P}_u}{\gamma R T_u} \qquad \rightarrow \qquad \Delta m_{valve} \approx -\frac{V_u}{\gamma R T_u} \Delta P_u \tag{9}$$

where $\Delta t$ is the duration of the discharge. Figure 3 (a) illustrates the experimental and theoretical air mass flow rates through one Pushpull inlet valve versus mark-space ratio for a number of upstream and downstream pressures. Both choked and nonchoked flow regimes can be observed. Figure 3 (b) presents the experimental flow results for the Vibrator outlet valve under only choked conditions.

Overall, the correlation between experiment and theory is very good. Similar accuracies were found for the Pushpull outlet and Vibrator inlet valves. Small discrepancies in the curvature of the experimental responses for the Pushpull inlet valve in Figure 3 (a) with respect to the theoretical curves were caused in part by inaccuracies in the instrumentation and in part by slight measurement errors in the upstream and downstream pressures during the tests. The discrepancies between theory and experiment in Figure 3 (b) for the Vibrator outlet valve at mark-space ratios above 80% and below 20% (circled on the figure) are thought to be caused by electromechanical limitations of the valves at the extreme mark-space ratios.

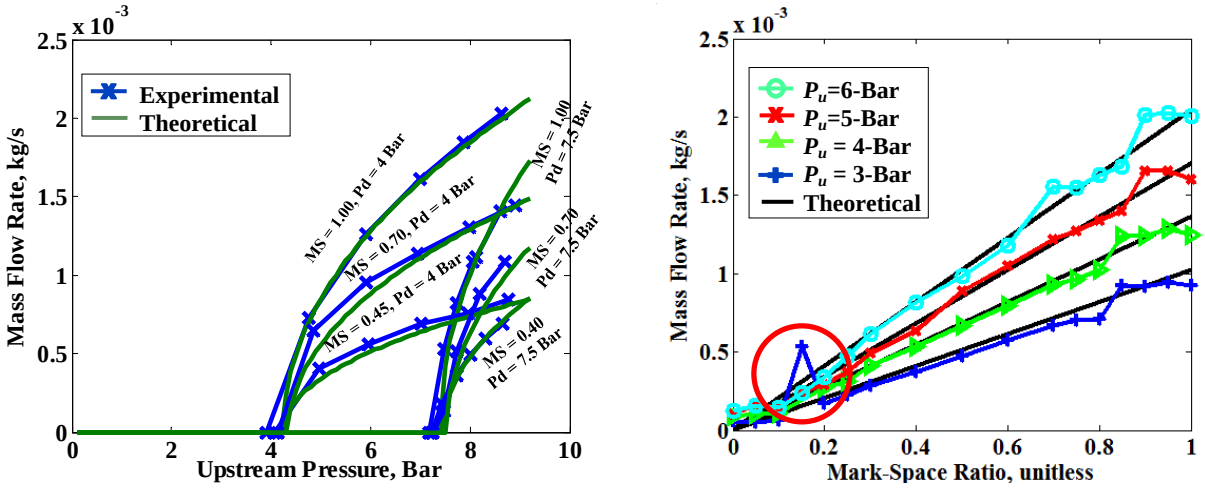


a) Experimental Choked and Nonchoked Mass Flow Rates through the Inlet Pushpull Valve

b) Experimental Choked Mass Flow Rates through the Outlet Vibrator Valve

**Figure 3 –**Flow Characterization of the Actuator

## 5. Simulating the Fill and Dump Pressure Transients

The equations of state of the chamber filling and dumping process are derived in this section. Equation (8) describes adiabatic flow into, or out of, a pressure vessel, and can be applied to brake chamber charging and discharging if the process is brief. If the process takes a long time, significant heat transfer can occur, and the process will be isothermal. Consider a control volume that encloses both the brake chamber and the mass of air entering or leaving the chamber. Assuming the system is isothermal and internally reversible, it can be shown using the Gibbs equations that

$$\dot{H} = 0 \qquad \rightarrow \qquad \dot{Q} = -V\dot{P} \tag{10}$$

with $H$ denoting the total enthalpy. Accordingly, Equation (7) becomes

$$(\dot{m}_{in} - \dot{m}_{out}) = \frac{V\dot{P}}{RT} + \frac{P\dot{V}}{RT} \tag{11}$$

Contrary to the derivation by Subramanian et al. (2004), (2006), the charge and discharge process of a brake chamber, as with many pressure vessels, tends to be polytropic of the form $PV^{\alpha}$ = const (Dutton, Coverdill, 1997). It follows that a more appropriate form for Equations (8) and (11) is (Richer, Hurmuzlu, 2000),

$$(\alpha_{in}\dot{m}_{in} - \alpha_{out}\dot{m}_{out}) = \frac{V\dot{P}}{RT} + \frac{\alpha_{cv}P\dot{V}}{RT} \tag{12}$$

where $\alpha$, $\alpha_{in}$, and $\alpha_{out}$ are experimentally determined coefficients that take values between 1 and $\gamma$, depending on whether the process is more isothermal or adiabatic respectively.

Equation (12) was used with Equations (2) and (3) to describe chamber charging and discharging by substituting $\dot{m}_{valve}$ for $\dot{m}_{in}$ or $\dot{m}_{out}$ respectively. A temperature sensor on the chamber revealed that the temperature varied by less than 5% during charging and discharging, and so $\alpha_{in}$ and $\alpha_{out}$ were taken to be 1. This agrees with the findings of Dutton and Coverdill (1997). Moreover, $\alpha_{cv}$ was taken to be 1.2 to describe the polytropic chamber compression-expansion process, as recommended by Richer and Hurmuzlu (2000).

A plot comparing the simulated pressures in the chamber during charging and discharging with experimental results using a brake chamber and the Camcon valves is shown in Figure 4. In general, the agreement between theory and experiment is very good. The measured rate of pressure drop is initially faster than the theoretical during discharging. This is likely due to a hysteresis in the volume change that was not observed during static volumetric measurements.

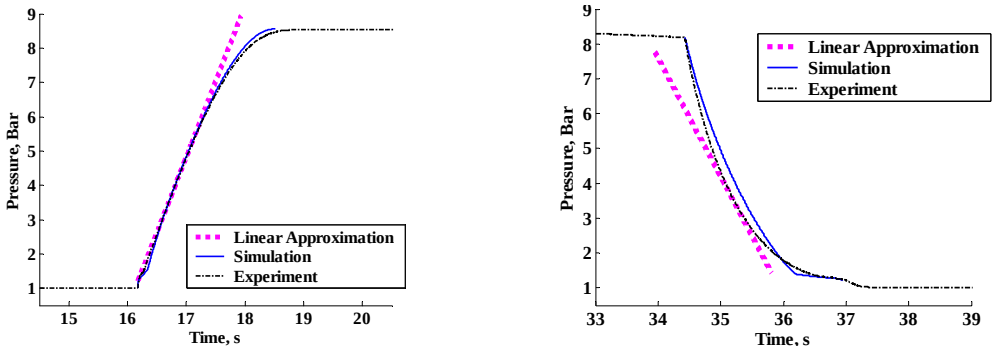


a) Charging b) Discharging

**Figure 4 –**Simulation of Chamber Pressure as a Function of Time

## 6. Open and Closed-Loop Characteristics of the Actuator

The operating point of the gain-scheduled wheel slip controller when coupled with conventional braking pneumatics on a HiL rig was approximately 3.5 Bar absolute (Kienhofer et al., 2007). Assuming that the upstream supply tank pressure is at least 7 Bar absolute, the flow into and out of the chamber will be choked. Equating Equation (2) to Equation (12) for chamber charging and rearranging,

$$\dot{P}_{cham} = \frac{C_f A_v C_1 \frac{P_u}{\sqrt{T}}}{\frac{V_{cham}}{\alpha_{in}RT} + \frac{\alpha_{cv}P_{cham}\frac{dV_{cham}}{dP_{cham}}}{\alpha_{in}RT}} MS \tag{13}$$

here the subscript *'cham'* indicates conditions in the brake chamber. Equation (13) may be used for discharging, but with $P_u$ replaced by $P_{cham}$, $\alpha_{in}$ replaced with $\alpha_{out}$, and the right side made negative.

Equation (13) is the pressure control system equation, with *MS* as the input, and $P_{cham}$ as the output. The system equilibrium point of interest is when the chamber pressure equals the desired pressure, here assumed to be 3.5 Bar absolute, and the mark-space ratio is zero. Linearizing Equation (13) about that point,

$$\dot{P}_{cham} = (const)MS \tag{14}$$

or, in other words, the plant may be approximated as an integrator. The linearized approximation to Equation (13) is shown on Figure 4, and it can be seen that this approximation is valid for a wide range of pressures during chamber charging, and an acceptable range of pressures for chamber discharging.

Purely proportional controllers are recommended for both type 1 systems and pressure control loops (Dutton, 1997). Consequently, a closed loop proportional control system was investigated. Analogue electronics were used to avoid quantization issues, so the limits of the valves could be explored. Experimental and simulated open loop and closed loop bode plots for one pushpull valve with gains of 1 and 7 are shown in Figure 5. The simulated plots were based on Equation (14). Again, there is very good agreement between the simulated and experimental results. Similar accuracies were found with all other valves.

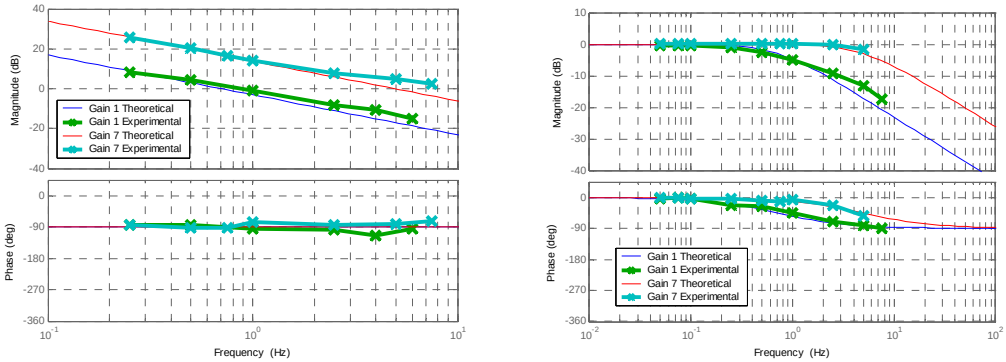


a) Open Loop Response b) Closed Loop Response

**Figure 5 –** Open and Closed Loop Bode Plots for the Valves

Theoretically, with an integrator as the plant, the gain on the proportional controller can be driven to infinity without the system becoming unstable. Though the stability margins of the valves remained high throughout their range of operation, the gain on the individual Pushpull valves could only be driven to 7, beyond which two issues arose. First, because of the 20 Hz PWM control frequency of the Pushpull valves, an aliasing effect prevented the valves from adequately following frequencies higher than 5 Hz, the approximate bandwidth attained with a gain of 7. Second, leakage through the valves upset the system for higher gains.

The gain on the Vibrator valves could be driven to 50, but this yielded a bandwidth of 9 Hz, well below the frequency where one would expect aliasing considering the valves' 250 Hz PWM drive frequency. The vibrator valves were limited by an acoustical pressure wave whose frequency corresponded to the Helmholtz resonant frequency of the brake chamber.

The wave dominated the chamber pressure signal at high switching frequencies, limiting the magnitude of the proportional gain.

The closed loop step response of all 6 valves working together to charge and discharge the chamber is shown in Figure 6. The Pushpull and Vibrator valves were used when the pressure error was greater than 25 mBar, and just the Vibrator valves were used when the error was less than 25 mBar. 4 mBar steady-state accuracies were seen. Furthermore, the speed of response of the valves was less than 5 ms, as compared to the lag of over 50 ms seen in similar tests performed with conventional ABS solenoid valves.

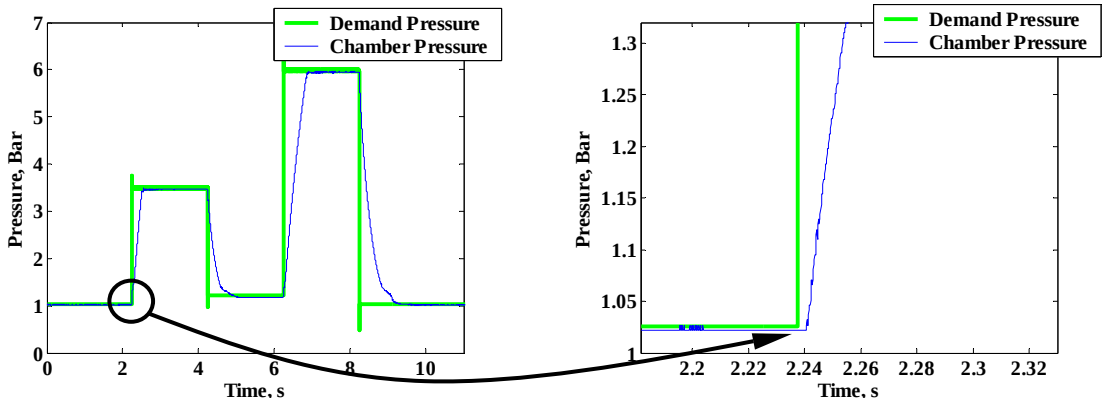


**Figure 6 –** Closed Loop Step Response with All 6 Valves

## 7. Conclusions

(1) To implement wheel slip control, and improve the stopping performance of HGV's, conventional braking hardware needs to be modified.
(2) The tradeoff between stopping distance and air usage needs to be considered in the design of a slip controller.
(3) A novel, fast acting brake actuator has been developed. The response of the actuator and the polytropic charging and discharging of the brake chamber was approximated with reasonable accuracy using 1-dimensional flow theory and basic thermodynamic arguments.
(4) The new actuator provided stable closed-loop pressure control. However, the controller gains were limited by the PWM frequency of the valves, leakage, and acoustical resonance in the brake chamber.

## 8. Acknowledgements

The authors would like to thank the members of the Cambridge Vehicle Dynamics Consortium (CVDC), Cambridge Commonwealth Trust, University of the Witwatersrand, Gates Cambridge Trust, and Churchill College for their parts in funding this work. At the time of writing, the CVDC had the following industrial members: ArvinMeritor, Camcon, Denby Transport, Firestone Industrial Products, Fluid Power Design, FM Engineering, Haldex, Mektronika Systems, MIRA, QinetiQ, Shell UK, Tinsley Bridge, and Volvo Trucks.

## 9. References

- Annon. (2006), “Traffic Safety Facts, 2005”, Washington, DC, National Highway Traffic Safety Administration, US Department of Transportation.

- Bowman, J. E., Law, E. H. (1993), “A Feasibility Study of an Automotive Slip Control Braking System”, SAE Journal (Transactions), (930762), 1166 – 1192.
- Bu, F., Tan, H. S. (2007), “Pneumatic Brake Control for Precision Stopping of Heavy-Duty Vehicles”, IEEE Transactions on Control Systems Technology, 15 (1), 53 - 63.
- Decker, H., Emig, R., Grauel, I., Engfer, O. (1986), “State of the Art and Future Prospects of Braking Control in Europe”, SAE Journal (Transactions), (861962), 988 - 994.
- Dugoff, H., Murphy, R. W. (1971), “The Dynamic Performance of Articulated Highway Vehicles - A Review of the State-of-the-Art”, SAE J. Transactions, (710223), 897-906.
- Dunn, A., Hoover, R. (2004), “Class 8 Truck Tractor Braking Performance Improvement Study, Report 1, Straightline Stopping Performance on a High Coefficient of Friction Surface”, East Liberty, OH, Transportation Research Center Inc. / National Highway Traffic Safety Administration.
- Dutton, C., Coverdill, R. (1997), “Experiments to Study the Gaseous Discharge and Filling of Vessels”, International Journal of Engineering Education, 13 (2), 123 - 134.
- Dutton, K. (1997), “The Art of Control Engineering”, Harlow, UK, Addison Wesley.
- Emereole, O. C. (2003), “Antilock Performance Comparison Between Hydraulic and Electromechanical Brake Systems”, Master’s Thesis in Mechanical and Manufacturing Engineering Science, University of Melbourne
- Fu, T. T., Cebon, D. (2003), “Economic Evaluation and the Design of Vehicle Suspensions”, International Journal of Vehicle Design, 31 (2), 125 - 161.
- Jiang, F., Gao, Z. (2001), “An Application of Nonlinear PID Control to a Class of Truck ABS Problems”, 40th IEEE Conference on Decision and Control (CDC), Orlando, FL.
- Kawabe, T., Nakazawa, M., Notsu, I., Watanabe, Y. (1997), “A Sliding Mode Controller for Wheel Slip Ratio Control System”, Vehicle System Dynamics, 27 (5 - 6), 393 - 408.
- Kienhofer, F. W., Cebon, D. (2004), “An Investigation of ABS Strategies for Articulated Vehicles”, 8th International Symposium on Heavy Vehicle Weights and Dimensions, Misty Hills, South Africa.
- Kienhofer, F. W., Miller, J. I., Cebon, D. (2007), “Design Concept for an Alternative Heavy Vehicle ABS System”, 20th IAVSD Symposium, Berkeley, CA.
- Kloeden, C. N., McLean, A. J., Glonek, G. (2002), “Reanalysis of Travelling Speed and the Risk of Crash Involvement in Adelaide South Australia”, Civic Square, ACT, Australian Transport Safety Bureau.
- Murphy, R. W., Limpert, R., Segel, L. (1970), “Bus, Truck, Tractor/Trailer Braking System Performance”, Ann Arbor, Michigan, Highway Safety Research Institute / National Highway Traffic Safety Administration / US Department of Transportation.
- Palkovics, L., Fries, A. (2001), “Intelligent Electronic Systems in Commercial Vehicles for Enhanced Traffic Safety”, Vehicle System Dynamics, 35 (4 - 5), 227 - 289.
- Peeta, S., Zhang, P., Zhou, W. (2005), “Behavior-Based Analysis of Freeway Car-Truck Interactions and Related Mitigation Strategies”, Transportation Research Part B – Methodological, 39 (5), 417 – 451.
- Richer, E., Hurmuzlu, Y. (2000), “A high performance pneumatic force actuator system: Part I - Nonlinear mathematical model”, ASME Journal of Dynamic Systems, Measurement, and Control, 122 (3), 416 - 425.
- Subramanian, S. C., Darbha, S., Rajagopal, K. R. (2004), “Modeling the Pneumatic Subsystem of an S-cam Air Brake System”, ASME Transactions, 126 (3), 36 - 46.
- Werde, J., Decker, H. (1992), “Brake by Wire for Commercial Vehicles”, SAE Journal (Transactions), (922489), 849 - 859.